Conf-750935--11

A COMPARISON OF DIFFERENTIAL AND INTEGRAL CROSS SECTION MEASUREMENTS

By

L. R. Greenwood, R. R. Heinrich & N. D. Dudey

For Presentation at
1st ASTM-Euratom Symposium on Reactor Dosimetry
Petten, Netherlands
September 22-25, 1975

MASTER

UofC-AUA-USERDA

ARGONNE NATIONAL LABORATORY, ARGONNE, ILLINOIS

operated under contract W-31-109-Eng-38 for the
U. S. ENERGY RESEARCH AND DEVELOPMENT ADMINISTRATION

I. Introduction

Neutron spectra of interest to reactor dosimetry are now routinely determined using spectral unfolding techniques, such as the SAND-II computer code. Integral saturated activities, determined by foil irradiations, are used to unfold the neutron spectra assuming that the appropriate nuclear cross sections are known. The accuracy of the unfolded spectra are thus directly related to the accuracy of tabulated cross sections, such as ENDF/B-IV.

In order to evaluate the accuracy of the nuclear cross sections, we have undertaken a program to simultaneously measure integral and differential cross sections. The method is to directly measure the differential neutron spectrum and compare this measured spectrum to the spectrum unfolded from integral multiple-foil reaction-rate measurements. Differences between the integral and differentially derived spectrum are due to (1) uncertainties in the reaction rate measurements, (2) the spectral unfolding algorithm, or (3) the differential cross section data. If errors in the first two factors are kept small and if this procedure were followed with several different neutron spectra, then the correct cross sections could, in principle, be unfolded. However, our primary goal is to establish the degree of consistency between integral and differentially derived spectra in order to determine the accuracy of integrally unfolded neutron spectra.

II. Experimental Procedure

Suitable neutron spectra can be generated by stopping a deuteron beam in a thick ^{9}Be foil. The $^{9}Be(d,n)$ reaction then produces a continuum of neutrons in a bell-shaped curve, peaking at a neutron energy that is about 40% of the incident deuteron energy.

A. Differential Measurements

The differential neutron spectra were measured using the time-of-flight technique with the pulsed deuteron beam from the Argonne tandem accelerator. Neutrons were detected using a NE213 (5 cm x 5 cm) liquid scintillator. Pulse shape discrimination was used to reduce the random gamma background. Neutron spectra were measured at incident deuteron energies of 14 and 16 MeV at angles of 0°-25°, with a flight path of 2.0 and 3.7 meters. Data of sufficient accuracy could be obtained in about 30 minutes of beam time.

The flight times were converted to neutron energies, and absolute neutron yields were calculated using detector efficiencies computed with a monte carlo code [1]. The total number of deuterons incident on the target was determined by charge integration.

The resultant spectra are shown in Figs. 1 and 2. The data agree quite well with measurements made by Weaver [2], as shown in Fig. 3, although our data include more angles and extend to lower neutron energies (0.8 MeV). Neutron spectra were actually measured as low as 200 keV. However, the

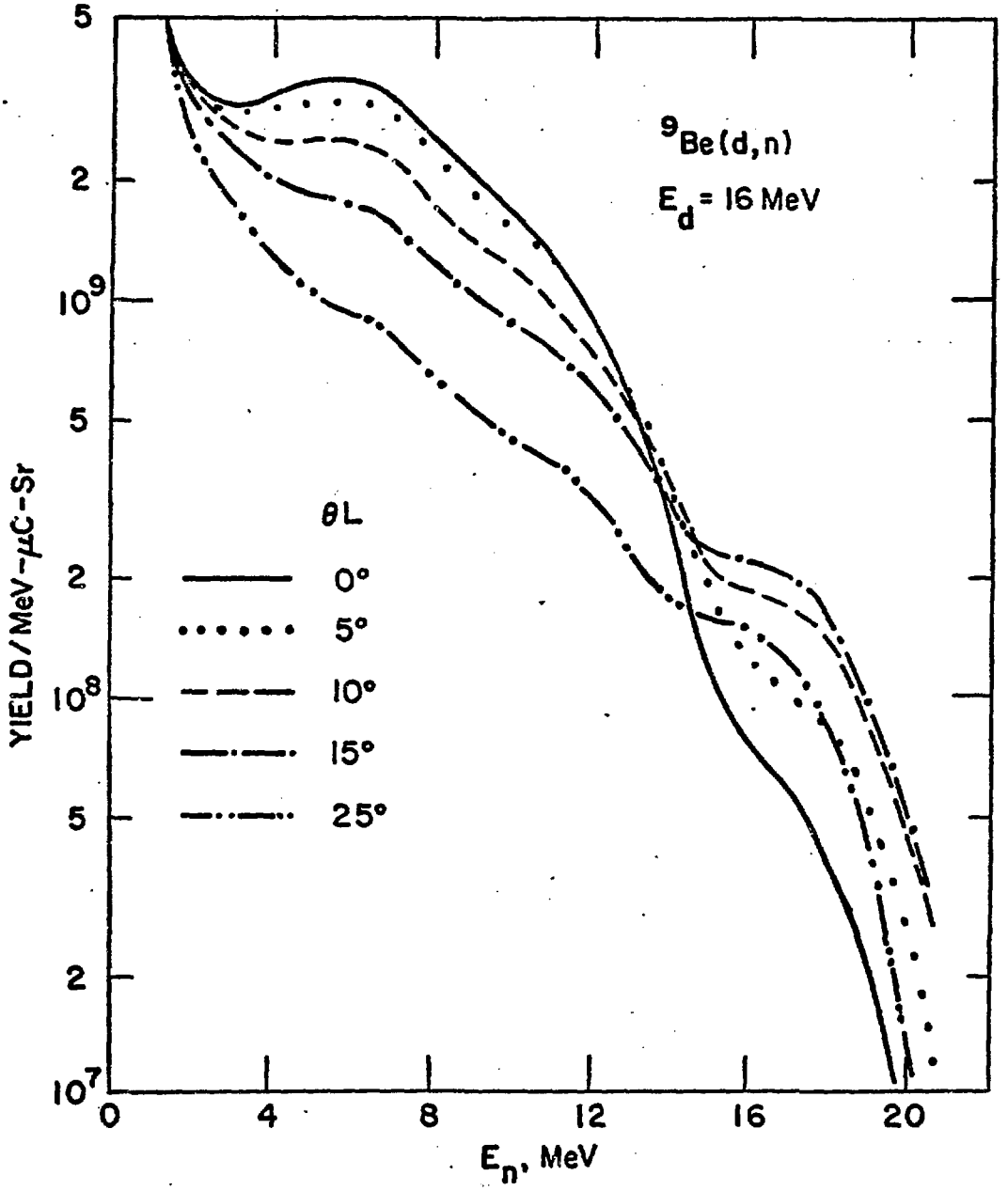

Fig. 1. ^{9}Be(d,n) Time-of-Flight Spectra are Shown at 16 MeV for 5 Angles

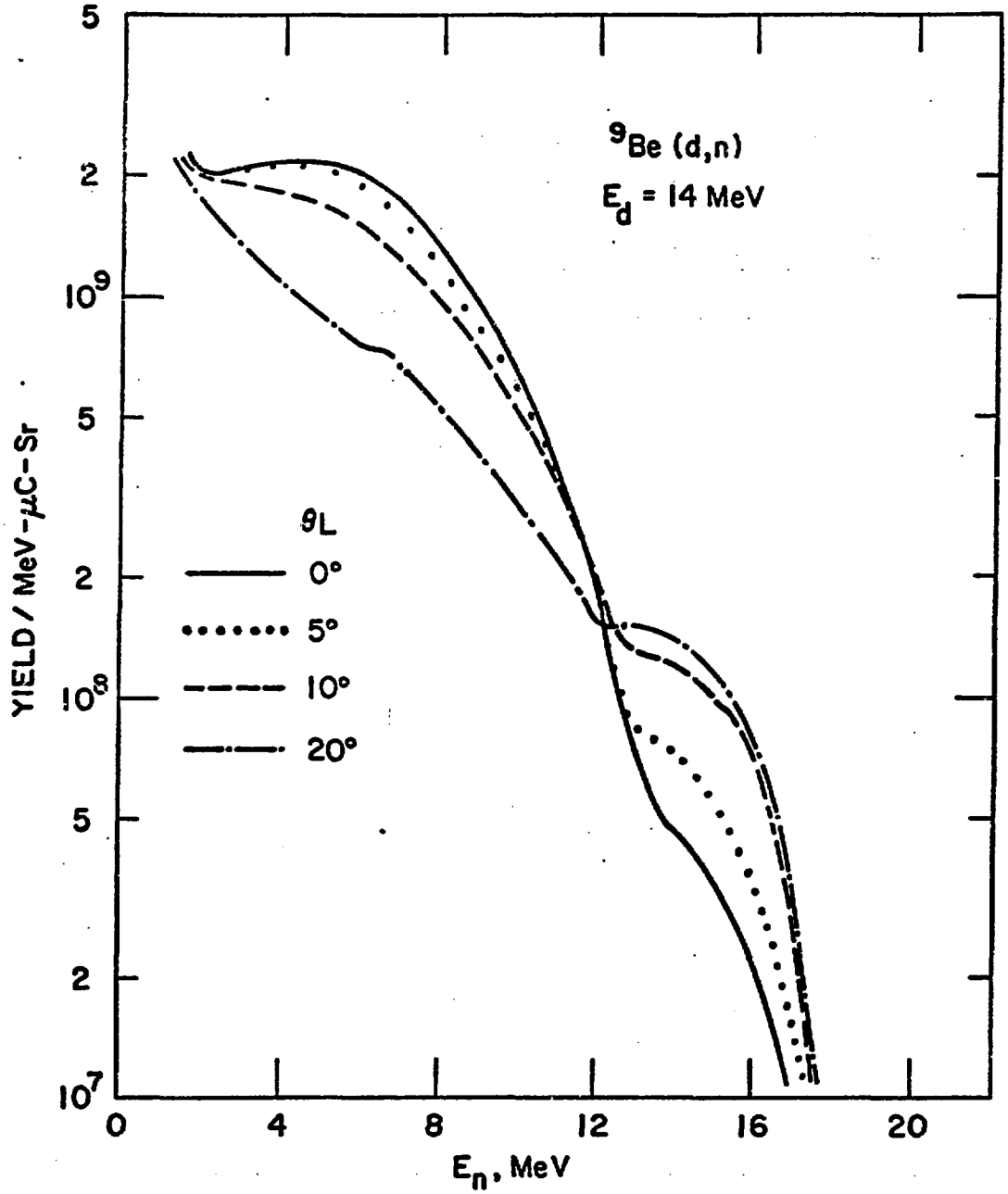

Fig. 2. ^{9}Be(d,n) Time-of-Flight Spectra are Shown at 14 MeV for 4 Angles

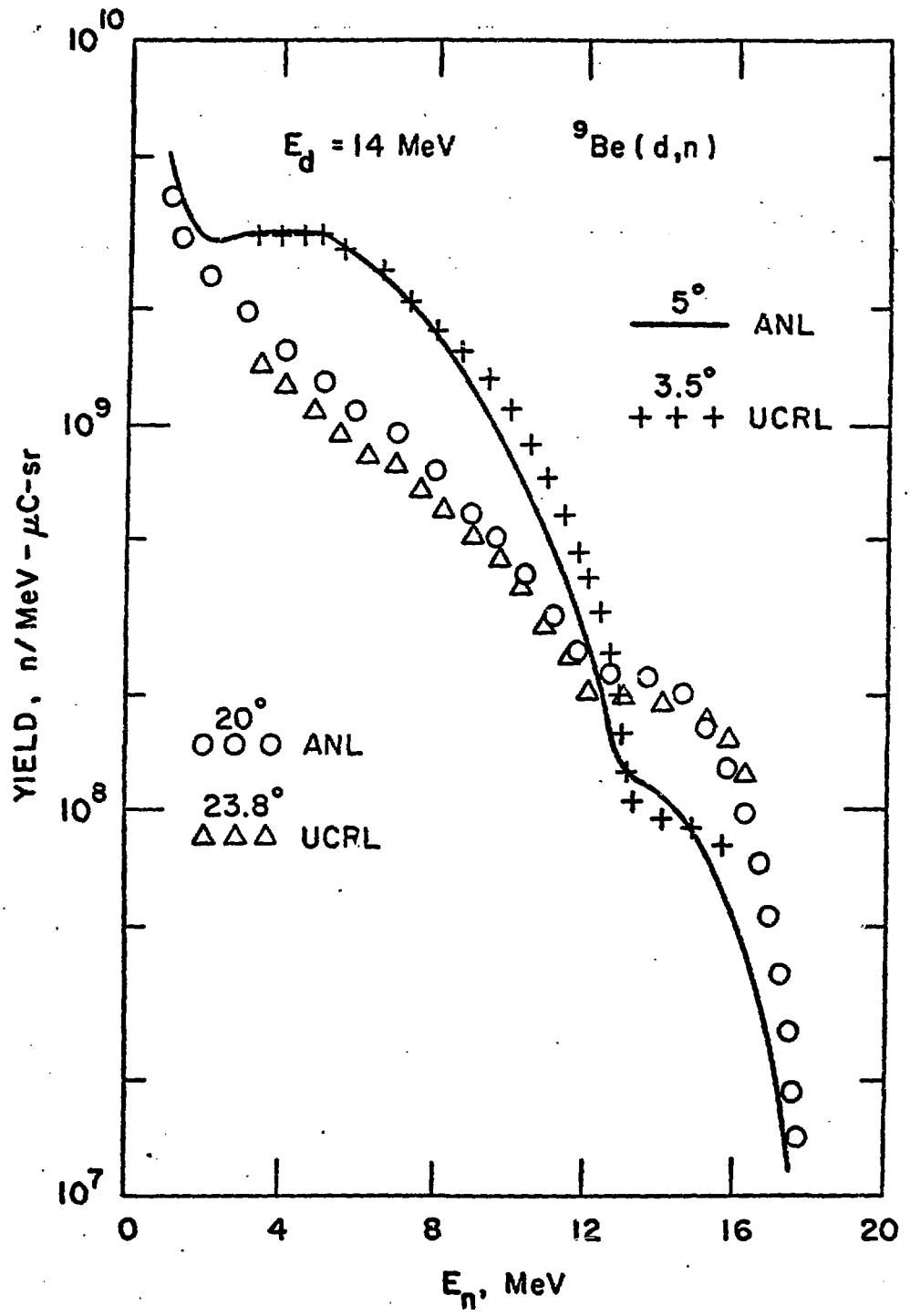

Fig. 3. Our Spectra at 14 MeV are Compared with Those of Weaver

calculated neutron efficiencies are not reliable in this region, and measurements of the efficiency in this region are now in progress.

B. Integral Activation Measurements

Foil packets consisting of Al, Au, Ni, Ti, ^{235}U, and ^{238}U were irradiated at 0° at E_d = 14 and 16 MeV. The foils were about 1 cm in diameter and were located about 4 cm from the center of the ^{9}Be target. In order to determine any variations in the spectra due to scattering or absorption effects, Au and Al foils were placed before and after each of the other materials. The ratios between the Al(n,α), Au(n,γ), and Au(n,2n) yields are highly sensitive to any spectral changes. A careful analysis of these results showed no deviation from the expected geometric effects ($1/R^2$), indicating that absorption and scattering effects were not significant.

The gamma yields from the irradiated foils were determined by Ge(Li) counting. All foils were measured at least twice in order to confirm the extrapolation to the end of irradiation time. Corrections were then made for decay during the irradiations, which lasted from 5-14 hours. The integrated beam current was recorded at 10 min intervals, and the decay correction was computed by summing the corrections for each short interval.

The resultant values of the saturated activities $\overline{\sigma\phi}$ were extracted for ten reactions. The natural Ti foil gives three contributions for the (n,p) reaction to ^{46}Sc, ^{47}Sc, and ^{48}Sc; however, corrections must be made for the (n,np) and (n,d) contributions to the activation products. For example, $^{46}Ti(n,p)$, $^{47}T(n,np)$, and $^{48}Ti(n,d)$ all lead to ^{46}Sc, although the latter two reactions only contribute at higher energies. This problem was handled by using the properly weighted activation cross sections in SAND-II.

The fission-foil values were averaged using ^{95}Zr, ^{103}Ru, and ^{140}Ba. However, fission yields are not known for our range of neutron energies ($\bar{E} \sim 5$-6 MeV) and had to be interpolated from the ENDF/B-IV values at 500 keV and 14 MeV. This resulted in fairly consistent saturated activities for the three fission products; however, the results are not as accurate as those for other reactions. In the future we intend to use a fission chamber of the NBS type in order to accurately determine the total fissions. Fission yields will then be deduced for our range of neutron energies.

III. Comparison of Differential and Integral Measurements

Since the foils subtended a finite range of angles (±7°), they saw a neutron spectrum given by an integral over the measured time-of-flight spectra. The uncertainty in the geometry is also worsened by the accelerator beam definition system. Any system of slits will produce a beam spot of finite size on the target and changes in the accelerator tuning conditions may cause this spot to wander on the target. An analysis of our system showed that this could have caused an error in our average irradia-

tion angle of as much as 1°. Any drift in the beam spot on the target produces a much larger shift in the average angle of irradiation since the foils are no longer concentric about 0°. This effect cannot be eliminated since the target-to-foil geometry must be close in order to produce a high neutron flux (*e.g.*, reducing the angle by a factor of 2 would have required extending the irradiation time by a factor of 4). However, we intend to reduce this effect in the future by redesigning the accelerator slit system.

For most of the reactions, the geometric effect is very small (<2%) and a properly averaged (by solid angle) neutron spectrum can be used. In our case, the 5° spectrum is quite close to the average. To be quite precise, each foil saw a slightly different average neutron spectrum since they were at slightly different distances; however, this effect is small, and simple corrections can be made to correct all integral values to the same irradiation geometry.

The case of the ^{58}Ni(n,2n) reaction is particularly striking and demonstrates that caution must be used in evaluating errors due to the geometry used in the foil irradiations. In this case, the high threshold energy makes the average activation cross section extremely sensitive to small changes in angle since the neutron flux is dropping rapidly at high energies and changes slope about 12-16 MeV (see Figs. 1 and 2). At E_d = 14 MeV, a change in the average irradiation angle of only ±1° would produce a change in the calculated saturated activity of ±15%. For all of the other reactions studied, this effect is less than ±3%. Hence, we have excluded the ^{58}Ni(n,2n) reaction from our comparisons and suggest that it be studied at higher incident deuteron energies.

The corrected activation results were finally compared with the time-of-flight data. The ratio of saturated activities ($\overline{\sigma\phi}$) are shown in Table I, where the numerator is the integrated foil data and the denominator is the averaged time-of-flight flux times the ENDF/B-IV activation cross section, integrated over energy. This ratio should be equal to one for total consistency between the integral and differential results, assuming that the nuclear cross sections are correct. Since the spectra were not measured below 0.8 MeV, the ^{197}Au(n,γ) calculation is somewhat sensitive to the assumption that one makes below this energy. We assumed that the flux was zero below E_n = 0.8 MeV in Table I. Other assumptions are discussed later (see Figs. 4 and 5).

As shown in Table I, the ratio of measured to calculated saturated activities has a standard deviation of ±14% at E_d = 16 MeV and ±28% at E_d = 14 MeV. It is interesting to note that the differences appear to be similar at both incident energies, that is, the ^{48}Ti(n,p) and ^{197}Au(n,2n) ratios are high and the fission products are low. These results, at present, provide only tentative information regarding the accuracy of the nuclear cross sections. Additional neutron spectra need to be examined and each of the measurements should be repeated for verification. The interpolated fission yields may be causing the apparent discrepancy for the fission reactions but this possibility is currently being investigated. Finally, we point out that the ^{197}Au(n,2n) reaction is also very sensitive to the high energy tail of the neutron spectra, although the sensitivity is much less than for the ^{58}Ni(n,2n) case.

TABLE I. Comparison of Saturated Activities for Integral (Foil) and Differential (TOF) Measurements

$$\text{Ratio} = \frac{\overline{\sigma\phi}(\text{foil})}{\int \sigma(\text{ENDF/B-IV})\,\phi(\text{TOF})\,dE}$$

Reaction	16 MeV	14 MeV
$^{197}Au(n,2n)^{196}Au$	1.14	1.36
$^{197}Au(n,\gamma)^{198}Au$	1.10[a]	1.09[a]
$^{27}Al(n,\alpha)^{24}Na$	0.96	0.96
$^{58}Ni(n,p)^{58}Co$	0.90	0.75
Ti → ^{46}Sc[b]	1.05	0.98
Ti → ^{47}Sc[b]	0.85	0.79
Ti → ^{48}Sc[b]	1.23	1.53
$^{238}U(n,f)$[c]	0.88	0.75
$^{235}U(n,f)$[c]	0.89[a]	0.79[a]
Std. Dev. (%)	13.5	28.2

[a] Below 0.8 MeV, $\phi(E)$ is assumed to be zero.

[b] (n,np) and (n,d) contributions included except for ^{49}Ti case.

[c] Average of ^{95}Zr, ^{103}Ru, and ^{140}Ba, using average fission yields from ENDF/B-IV.

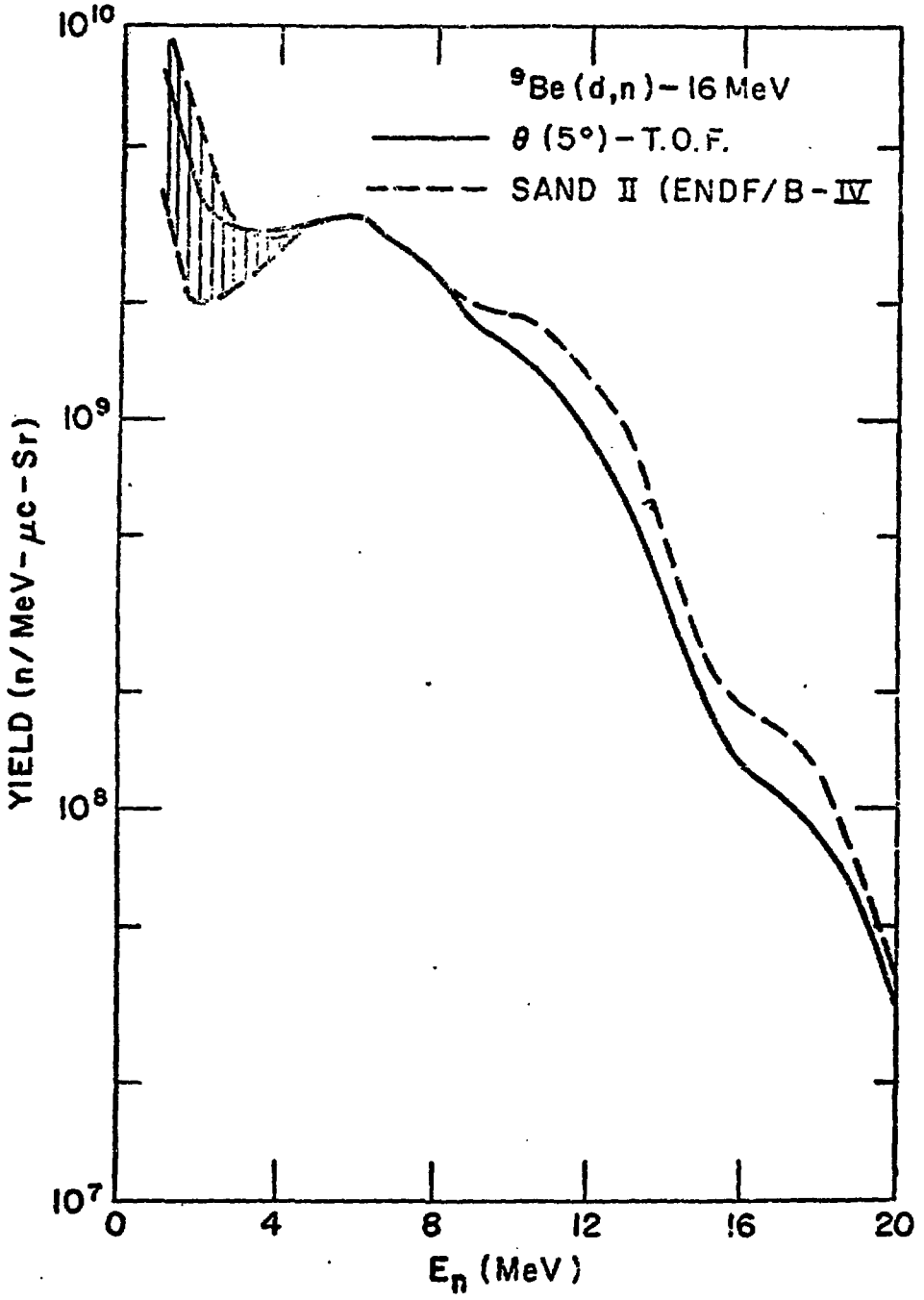

Fig. 4. Iterated SAND-II Spectrum at 16 MeV is Compared with the Average Time-of-Flight Spectrum

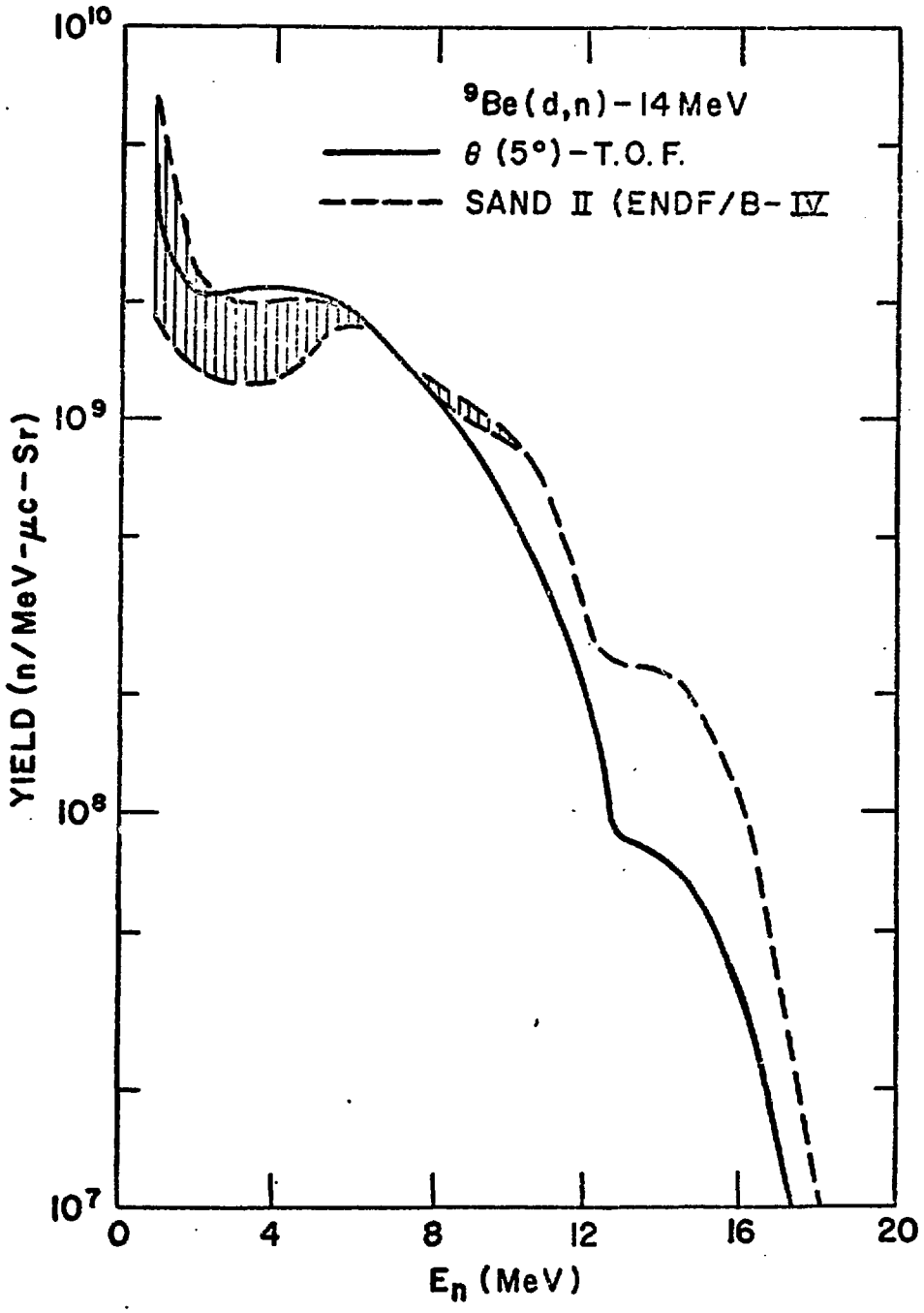

Fig. 5. Iterated SAND-II Spectrum at 14 MeV is Compared with the Average Time-of-Flight Spectrum

In order to examine the consistency between integral and differential spectrum measurement procedures, we used the measured activities to unfold the neutron spectra. These are compared to the time-of-flight spectra in Figs. 4 and 5. The banded regions at low energy reflect the uncertainty in the starting spectra (TOF) since our measurements did not extend below 0.8 MeV. Only the $^{197}Au(n,\gamma)$ calculations are very sensitive in this region and the data suggest that the flux is fairly low in this low energy region. The SAND-II multiple-foil unfolded spectrum is considerably more consistent with the measured reaction rates but this is expected because the spectrum is derived in a manner to force consistency. For this reason, comparisons as in Table I provide the most insight into differential and integral cross section consistency.

The results presented are certainly not adequate to make definitive statements regarding cross section inconsistencies. Our purpose, however, is to point out the approach and the type of work being carried out to assess cross section limitations in deriving high energy neutron spectra by the foil-activation spectral-unfolding technique. Our work is continuing to (1) improve upon the accuracy of the time-of-flight spectral measurements, (2) derive energy dependent fission yields for the fission reactions, (3) obtain activation rate data for more reactions in order to expand the number of cross sections which can be studied, and (4) improve the quality of accelerator-produced neutron spectra.

REFERENCES

[1] POENITZ, W.P., "The Black Neutron Detector," ANL-7915 (1972).

[2] WEAVER, K.A., "Spectra of Neutrons From Deuteron Bombardment of Light Nuclei," UCRL-51310 (Addendum) (1973).

Figure Captions

Fig. 1 $^{9}Be(d,n)$ Time-of-Flight Spectra are Shown at 16 MeV for 5 Angles

Fig. 2 $^{9}Be(d,n)$ Time-of-Flight Spectra are Shown at 14 MeV for 4 Angles

Fig. 3 Our Spectra at 14 MeV are Compared with Those of Weaver

Fig. 4 Iterated SAND-II Spectrum at 16 MeV is Compared with the Average Time-of-Flight Spectrum

Fig. 5 Iterated SAND-II Spectrum at 14 MeV is Compared with the Average Time-of-Flight Spectrum